



## Novel cinnoline-based inhibitors of LRRK2 kinase activity

Albert W. Garofalo<sup>a,\*</sup>, Marc Adler<sup>b</sup>, Danielle L. Aubele<sup>a</sup>, Simeon Bowers<sup>a</sup>, Maurizio Franzini<sup>a</sup>, Erich Goldbach<sup>c</sup>, Colin Lorentzen<sup>c,†</sup>, R. Jeffrey Neitz<sup>a,‡</sup>, Gary D. Probst<sup>a</sup>, Kevin P. Quinn<sup>c</sup>, Pam Santiago<sup>c</sup>, Hing L. Sham<sup>a</sup>, Danny Tam<sup>d</sup>, Anh P. Truong<sup>a</sup>, Xiaocong M. Ye<sup>a</sup>, Zhao Ren<sup>d</sup>

<sup>a</sup> Department of Medicinal Chemistry, Elan Pharmaceuticals, 180 Oyster Point Blvd, South San Francisco, CA 94080, United States

<sup>b</sup> Department of Molecular Design, Elan Pharmaceuticals, 180 Oyster Point Blvd, South San Francisco, CA 94080, United States

<sup>c</sup> Department of Drug Metabolism and Pharmacokinetics, Elan Pharmaceuticals, 180 Oyster Point Blvd, South San Francisco, CA 94080, United States

<sup>d</sup> Department of Assay Development, Elan Pharmaceuticals, 180 Oyster Point Blvd, South San Francisco, CA 94080, United States

### ARTICLE INFO

#### Article history:

Received 9 September 2012

Revised 31 October 2012

Accepted 7 November 2012

Available online 16 November 2012

#### Keywords:

LRRK2

Leucine rich repeat kinase 2

Parkinson's disease

Kinase inhibitors

### ABSTRACT

Leucine rich repeat kinase 2 (LRRK2) has been implicated in the pathogenesis of Parkinson's disease (PD). Inhibition of LRRK2 kinase activity is a therapeutic approach that may lead to new treatments for PD. Herein we report the discovery of a series of cinnoline-3-carboxamides that are potent against both wild-type and mutant LRRK2 kinase activity in biochemical assays. These compounds are also shown to be potent inhibitors in a cellular assay and to have good to excellent CNS penetration.

© 2012 Elsevier Ltd. All rights reserved.

Since the identification of the Park8 gene,<sup>1</sup> evidence has been mounting that implicates LRRK2 in the pathogenesis of Parkinson's disease (PD). At least five causal mutations in LRRK2 have been identified.<sup>2</sup> Of those, the G2019S mutation is the most prevalent amino acid substitution being found in ~5% of hereditary and 1–2% of idiopathic PD patients.<sup>3,4</sup> This prevalence rises to much higher levels in certain ethnic populations. The G2019S mutation is located in the kinase domain of LRRK2 and has been observed to cause an increase in kinase activity.<sup>5–7</sup> This increased kinase activity leads to broad neurotoxicity in both cellular and in vivo models thus providing strong experimental evidence that supports LRRK2 as a potential therapeutic target for PD.

We employed a kinase-inhibitor-focused screen of our in-house library as an expedient way to find LRRK2 inhibitor chemotypes. The screen used an HTRF assay measuring the inhibition of phosphorylation of LRRKtide.<sup>8</sup> A series of 4-aminoquinoline-3-carboxamides (e.g., **1** and **2**) were identified as LRRK2 inhibitors (Fig. 1). The in vitro potency of **2** was encouraging and the large difference in potency accompanying changes in substitution at C4 suggested a manipulable SAR. However, compounds of this type are known

CSF1R inhibitors<sup>9</sup> and in-house studies indicated that they were substrates for P-gp and had poor CNS uptake. We were therefore pressed to incorporate unique structural changes that would impart selectivity and improve the DMPK characteristics.

One approach that was examined involved replacing the quinoline core with cinnoline. We reasoned that introduction of nitrogen at C2 might improve CNS penetration by providing an additional intramolecular hydrogen bond with the amide.<sup>10</sup> These compounds were generally prepared as shown in Scheme 1. Addition of cyanoacetamide to the diazonium salt of 3-iodoaniline (**3**) afforded diazene **4**. AlCl<sub>3</sub>-promoted cyclization in toluene, in a sealed tube, at 150 °C produced cinnoline **5** which was converted to chloroamide **7** using a 3-step sequence.<sup>11</sup> Addition of isopropylamine followed by a Suzuki coupling gave the target cinnoline **11**.

LRRK2 in vitro assay results from the quinoline inhibitors suggested that substitution at C4 with small alkyl amines was preferred. The biochemical potencies for several analogs with differing C4 alkyl substitution in the cinnoline series are listed in Table 1. In general, wild-type potencies paralleled G2019S potencies, although with slightly lower IC<sub>50</sub> values. A notable exception is compound **20** which exhibited better potency against the mutant enzyme. Interestingly, homologation by a single carbon, compound **16**, reversed this selectivity. In vitro potency was greatest with small, lipophilic amines at this position and the introduction of a chiral center positively impacted the biochemical potency (cf. **13** and **15**). Compounds **12** and **13** are two of the most potent compounds that we prepared. We had previously observed a eudismic

\* Corresponding author.

E-mail address: [albert.garofalo@elan.com](mailto:albert.garofalo@elan.com) (A.W. Garofalo).

† Present address: Novartis Institutes for Biomedical Research, Emeryville, CA 94608, United States.

‡ Present address: Small Molecule Discovery Center, Univ. of California-San Francisco, San Francisco, CA 98158, United States.

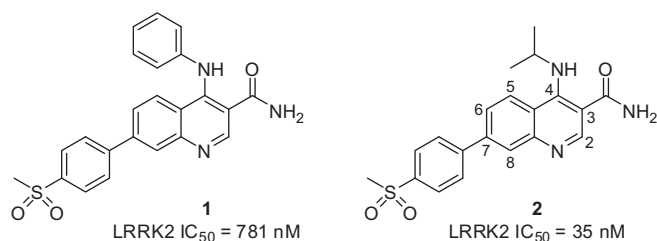
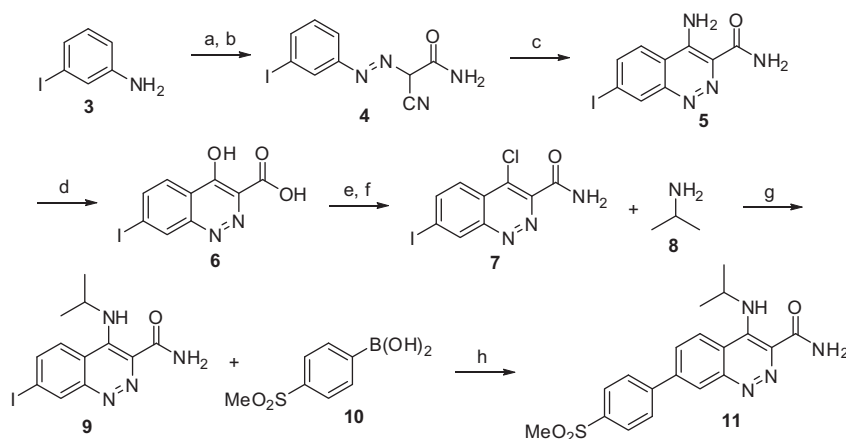


**Figure 1.** Initial screening hits.

ratio (*R/S*) of 10 for chiral amines in the quinoline series (data not shown) and prepared only the (*R*)-enantiomers in the cinnolines. This seemed reasonable given the similar presumed hinge binding orientations of both series (*vide infra*).

We developed a homology model of LRRK2 based on MLK1 (pdb ID: 3DTC).<sup>12</sup> At the time, the 3DTC structure had the closest

homology to LRRK2 as judged by the BLAST score ( $1e-25$ , with 31% identities). However, the 3DTC contained several ligand induced conformational changes that were undesirable. These included a collapsed P-loop and a partially disordered DFG sequence. The P-loop was remodeled using homologous structures of kinases with ATP analogues. The DYG sequence was built to resemble PKC- $\iota$  (pdb ID: 3A8X), one of the few pdb kinase structures that contain a DYG sequence.<sup>13</sup> Docking of compound **11** into this model shows a two-point hinge interaction with N1 of the cinnoline accepting a hydrogen bond from A1950 and the carboxamide donating a hydrogen bond to E1948 (Fig. 2). This model shows the C7 substituent pointing out toward the solvent channel. Based on this model several analogs with varying substitution at C6 and C7 were examined (Table 2). We observed only small differences in *in vitro* potency with identical substituents at either C6 or C7 as would be expected for this region of the molecule (cf. **27** and **25**, **28** and **29**, **30** and **31**).



**Scheme 1.** Reagents and conditions: (a)  $\text{NaNO}_2$ , 6 N HCl; (b) NaOAc,  $\text{NCCH}_2\text{CONH}_2$  (78%, 2 steps); (c)  $\text{AlCl}_3$ , toluene,  $150^\circ\text{C}$  (95%); (d) KOH, dioxane,  $110^\circ\text{C}$ ; (e)  $\text{SOCl}_2$ ; (f)  $\text{NH}_4\text{OH}$  (45%, 3 steps); (g) EtOH,  $140^\circ\text{C}$  (47%); (h)  $\text{Pd}(\text{PPh}_3)_4$ ,  $\text{K}_2\text{CO}_3$ , dioxane,  $\text{H}_2\text{O}$  (70%).

**Table 1**  
Inhibitory activity against wild-type (wt) and mutant G2019S LRRK2

Compound	Series	R	LRRK2 (wt) $\text{IC}_{50}$ ( $\mu\text{M}$ )	LRRK2 (G2019S) $\text{IC}_{50}$ ( $\mu\text{M}$ )
11	A	Isopropyl	0.015	0.027
12	A	( <i>R</i> )- <i>sec</i> -Butyl	0.001	0.004
13	A	( <i>R</i> )-1-Cyclopropylethyl	0.001	0.007
14	A	Cyclobutyl	0.010	0.019
15	A	Cyclopropylmethyl	0.017	0.027
16	A	Ethyl	0.046	0.055
17	A	Tetrahydropyran-4-yl	0.023	0.032
18	A	Cyclopropyl	0.049	0.052
19	A	(+/-)-Tetrahydrofuran-3-yl	0.017	0.053
20	A	Methyl	0.119	0.056
21	A	H	0.142	0.298
22	A	( <i>R</i> )-1-Phenylethyl	0.965	1.495
23	B	3-Hydroxypropyl	0.121	0.162
24	B	3-Hydroxyethyl	0.145	0.264
25	B	Isopropyl	0.015	0.016
26	B	( <i>R</i> )-1-Cyclopropylethyl	0.002	0.006

Enzyme activity was determined using GST-LRRK2 (970–2527), GST-(G2019S) LRRK2 (970–2527), and LRRKtide in the presence of 100  $\mu\text{M}$  ATP.

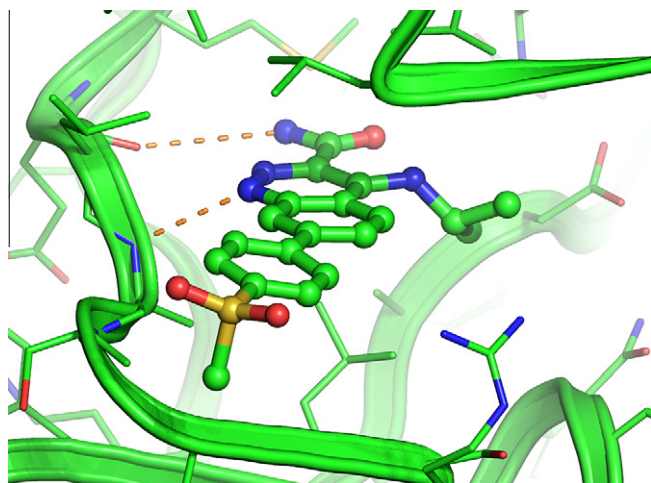
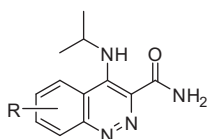


Figure 2. LRRK2 homology model with compound **9** docked.

Table 2  
Inhibitory differences with substitution at C6 and C7



Compound	R	LRRK2 (wt) IC <sub>50</sub> (μM)	LRRK2 (G2019S) IC <sub>50</sub> (μM)
<b>27</b>	6-(Pyridin-4-yl)	0.030	0.066
<b>25</b>	7-(Pyridin-4-yl)	0.015	0.016
<b>28</b>	6-(1 <i>H</i> -Pyrazol-4-yl)	0.001	0.005
<b>29</b>	7-(1 <i>H</i> -Pyrazol-4-yl)	0.012	0.018
<b>30</b>	6-(1-Methylpyrazol-4-yl)	0.378	0.425
<b>31</b>	7-(1-Methylpyrazol-4-yl)	0.009	0.012
<b>32</b>	7-(4-Methylpiperazin-1-yl)	0.053	0.059
<b>33</b>	7-(4-Morpholinophenyl)	0.009	0.012
<b>34</b>	7-(Thiazol-4-yl)	0.014	0.020

Additionally, we tested a few *N*-methylamides as well as substitution at C8 (Fig. 3). Secondary amides were substantially less potent, likely due to a steric interaction with the methionine gatekeeper. As expected substitution at C8 was not tolerated due to the proximity of this position with the hinge.

We were interested in obtaining a cellular measurement of the ability of these compounds to inhibit LRRK2 kinase activity. It has been demonstrated that inhibition of LRRK2 kinase decreases phosphorylation of S935 and that this decreased phosphorylation can be used as a measure of LRRK2 kinase activity.<sup>14</sup> Our cellular assay employed HEK293 cells stably transfected with LRRK2 (G2019S). Several compounds exhibited better than 100 nM potency and we observed good correlation with in vitro results (Table 3).

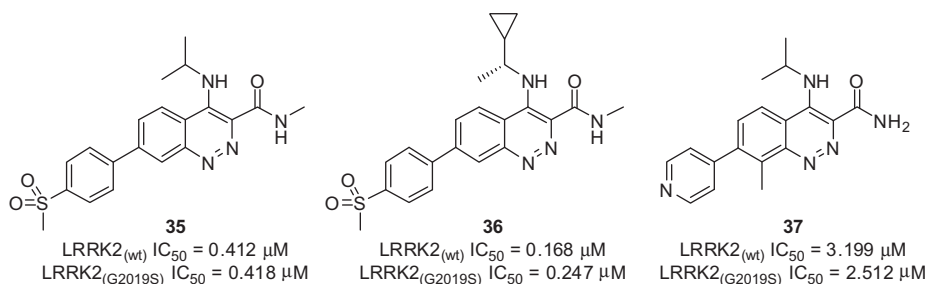


Figure 3. Lower in vitro potencies observed with *N*-methylamides and methyl substitution at C8.

Table 3  
Cellular potencies

Compound	LRRK2 (G2019S) EC <sub>50</sub> (μM)
<b>11</b>	0.218
<b>12</b>	0.073
<b>13</b>	0.070
<b>25</b>	0.242
<b>26</b>	0.062
<b>28</b>	0.109
<b>34</b>	0.290

Table 4  
Inhibitory activity against CSF1R and PDGFRα

Compound	CSF1R IC <sub>50</sub> (μM)	PDGFRα IC <sub>50</sub> (μM)
<b>13</b>	0.017	0.054
<b>14</b>	<0.040	0.022
<b>11</b>	0.012	0.127
<b>33</b>	0.022	0.262

CNS distribution of compounds was evaluated in both the Mdr1 a/b (−/−) and P-gp competent wild-type FVB mice to obtain in vivo P-gp efflux and brain uptake results. Gratifyingly, good to excellent CNS penetration was observed at 5 min following a 1 mg/kg IV dose. Penetration was assessed from the brain concentration to plasma concentration ratios (*K<sub>p</sub>*) in the wild-type mice and was 0.76, 1.50 and 11.4 for compounds **14**, **26** and **33**, respectively. Negligible in vivo P-gp efflux was also measured and was consistent with values obtain in vitro from MDR1-MDCK transfected cells.

We selected several potent compounds for selectivity screening against a panel of 40 kinases.<sup>15</sup> Unfortunately we were disappointed to find that most of the compounds tested were fairly promiscuous kinase inhibitors. Inhibition of both CSF1R and PDGFRα was of particular concern and dose responses were determined for these kinases to confirm the observations of the broad selectivity screen (Table 4).<sup>16</sup> Another clear result from this screen was that analogs substituted at C6 as opposed to C7 were much more promiscuous inhibitors.

In summary, we have designed and synthesized a novel series of cinnoline carboxamides that are potent and CNS penetrant LRRK2 inhibitors. A homology model of LRRK2 binding was developed and an inhibitor binding mode postulated based on this model. Close interactions indicated by the model were tested by the preparation of specific analogs. However, the inhibitors presented here exhibited less than desirable kinase specificity and as a result further medicinal chemistry efforts have been suspended.

#### Acknowledgments

The authors thank Wayman Chan (Elan) for performing difficult purifications. We would also like to acknowledge the work of

Pui Seto, Monica You, Jeanne Baker, and Kevin Tanaka for the production and purification of antibodies used in our assays.

### Supplementary data

Supplementary data associated with this article can be found, in the online version, at <http://dx.doi.org/10.1016/j.bmcl.2012.11.021>.

### References and notes

1. Funayama, M.; Hasegawa, K.; Kowa, H., et al *Ann. Neurol.* **2002**, *51*, 296.
2. Greggio, E.; Cookson, M. R. *ASN Neurochem.* **2009**, *1*, 13.
3. Healy, D. G.; Falchi, M.; O'Sullivan, S. S., et al *Lancet Neurol.* **2008**, *7*, 583.
4. Latourell, J. C.; Sun, M.; Lew, M. F., et al *BMC Med.* **2008**, *6*, 32.
5. West, A. B.; Moore, D. J.; Biskup, S., et al *Proc. Nat. Acad. Sci.* **2005**, *102*, 16842.
6. Greggio, E.; Jain, S.; Kingsbury, A., et al *Neurobiol. Dis.* **2006**, *23*, 329.
7. Jaleel, M.; Nichols, R. J.; Deak, M., et al *Biochem. J.* **2007**, *405*, 307.
8. Homogeneous time-resolved fluorescence (HTRF) assay using GST-LRRK2. Detection was done using biotinylated LRRKtide, Eu(K)-Ab (*p*-Moesin)/SA-XL665 measured at 620 and 665 nm.
9. Smalley, T. L., Jr.; Chamberlain, S. D.; Mills, W. Y., et al *Bioorg. Med. Chem. Lett.* **2007**, *17*, 6257.
10. It has been speculated that intramolecular hydrogen bonds can account for the high permeability of compounds with non-optimal physicochemical properties. See: Alex, A.; Millan, D. S.; Perez, M., et al *Med. Chem. Commun.* **2011**, *2*, 669.
11. Scott, D. A.; Dakin, L. A.; Del Valle, D. J., et al *Bioorg. Med. Chem. Lett.* **2011**, *21*, 1382.
12. Hudkins, R. L.; Diebold, J. L.; Tao, M., et al *J. Med. Chem.* **2008**, *51*, 5680.
13. Takimura, T.; Kamata, K.; Fukasawa, K., et al *Acta Crystallogr. D. Biol. Crystallogr.* **2010**, *D66*, 577.
14. Dzamko, N.; Deak, M.; Hentati, F., et al *Biochem. J.* **2010**, *430*, 405.
15. Compounds were profiled at Invitrogen in a single-point assay (see Supplementary data).
16. Dose responses for CSF1R and PDGFR $\alpha$  were generated in-house using a peptide-based TR-FRET assay in the presence of 1 mM ATP.